2009 International Symposium on Nonlinear Theory and its Applications
NOLTA'09, Sapporo, Japan, October 18-21, 2009

Experimental manipulations of intrinsic localized mode in macro-mechanical cantilever array toward micro-system

Masayuki Kimura† and Takashi Hikihara‡

†Department of Electronic Systems Engineering, The University of Shiga Prefecture
2500 Hassaka-cho, Hikone, Shiga 522-8533 Japan
Email: kimura.m@e.usp.ac.jp
‡Department of Electrical Engineering, Kyoto University
Katsura, Nishikyo, Kyoto 615-8510 Japan
Email: hikihara@kuee.kyoto-u.ac.jp

Abstract—A macro-mechanical cantilever array is newly proposed for experimental investigations of intrinsic localized modes (ILMs). The cantilever array is designed to have individually tunable on-site potentials. Thus, impurities in the array can be induced and removed manually. By a sinusoidal excitation, several ILMs are successfully generated. In addition, the generated ILM is manipulated by adding an impurity to the cantilever array. The mechanism of the manipulation is numerically discussed based on the structure of phase space. Coexisting ILMs, unstable manifolds, and domains of attraction of stable ILM are shown for the case that an ILM is manipulated by adding an impurity.

1. Introduction

An energy localization in discrete media is called intrinsic localized mode (ILM). A. J. Sievers and S. Takeno first discovered ILM as a spatially localized and temporally periodic solution in a nonlinear discrete lattice [1]. In this decade, ILMs have been identified in micro- or nano-systems. These experimental studies directly suggest the phenomenological universality of ILM. In addition, the experiments in micro-cantilever arrays [2, 3] allow us to expect to apply ILM to micro- or nano-engineering. Because cantilever structures are widely used in micro- and nano-devices [4]. Thus, ILM in a micro-cantilever array will have a potential to be utilized for sensors and actuators which have high sensitivity and accuracy.

For applications of ILM, it is necessary to establish a control method. That is, ILM has to be generated, destroyed, and moved as desired. An experimental manipulation in micro-cantilever arrays has been realized by M. Sato [5]. ILMs are generated, destroyed, repelled, and attracted by adding a localized impurity. It implies that a control method can be established based on the manipulation using impurities.

To establish the control method, it is necessary to clarify a mechanism of the manipulation. In addition, experimental investigations are inevitable to confirm the grasped mechanism. For the purpose, a macro-system shows the advantage to confirm the dynamics and the principles of the control method. Then a macro-system is proposed as an analogous dynamical model to the micro- or nano-system, so that the dynamical behaviors can be discussed experimentally.

One of the good analogous models is a magneto-elastic beam system [6]. The experimental model has a similar equation of motion to the micro-cantilever array in which ILMs were observed. In the model, permanent magnets are placed to adjust the on-site nonlinearity. If the magnetic field is adjustable at each site, it will be possible to add or release an impurity. Along the idea, we designed a macro-mechanical cantilever array having tunable electromagnets based on the magneto-elastic beam system. In this paper, at first, the macro-mechanical cantilever array is introduced and is modeled as nonlinear coupled ordinary differential equations. Then an experimentally observed ILM is shown with a numerical simulation. In addition, an attractive manipulation is demonstrated. In Sec. 4, the phase structure around the manipulated ILM is investigated numerically. Finally, the experimental attraction is numerically confirmed.

2. Macro-mechanical Cantilever Array

In this section, a macro-mechanical cantilever array is introduced and model equations are described. A schematic configuration of the macro-mechanical cantilever array is shown in Fig. 1 (a). The array consists of eight cantilevers, permanent and electro magnets (PM and EM), a coupling rod, and a voice coil motor. The cantilevers are placed with an equal interval of 15.0 mm in one dimension. The size of each cantilever is 70.0 mm in length, 5.0 mm in width, and 0.3 mm in thickness. At the free end of each cantilever, a small cylindrical PM is attached to face the EM which is placed beneath the cantilever. Because of the magnetic interaction between these magnets, each cantilever is governed by a nonlinear restoring force against the displacement of its tip.

The magnetic force between PM and EM can approximately be described by Coulomb's law for magnetic charges. Then the interaction force is nonlinearly changed against the displacement of cantilever. The configuration of magnetic charges is shown in Fig. 1 (b). If the displacement of cantilever is sufficiently small relative to the length of cantilever, Coulomb's law for magnetic charges gives

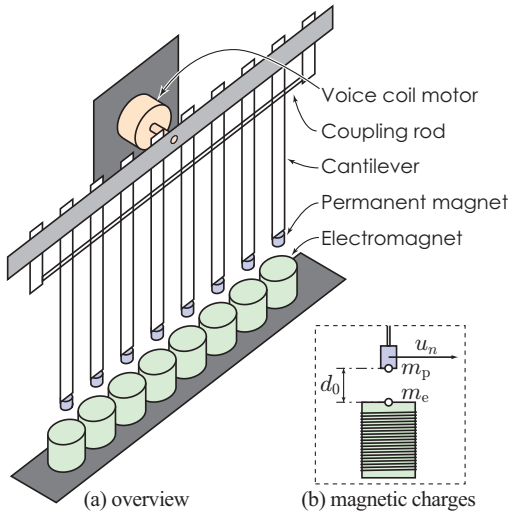

Figure 1: Configuration of (a) cantilever array and (b) magnetic charges.

Table 1: Parameter symbols and their estimated values in Eq. (2)

Symbol	Value	Symbol	Value
ω_0	$2\pi\times35.1$ rad/s	γ	1.5 s^{-1}
C	284 s^{-2}	χ_0	-4.71×10^{-5} m^3/s^2
d_0	3.0 mm	χ_1	-9.14×10^{-3} m^3/s^2A
A	3.0 m/s^2	ω	$2\pi\times36.1$ rad/s

the restoring force

$$F(u_n) = \frac{m_p m_e}{4\pi\mu_0}\frac{u_n}{\left(u_n^2+d_0^2\right)^{\frac{3}{2}}} = \chi(I_{EM})\frac{u_n}{\left(u_n^2+d_0^2\right)^{\frac{3}{2}}}, \quad (1)$$

where m_p and m_e correspond to magnetic charges of PM and EM, respectively. The distance between PM and EM at the equilibrium state is denoted by d_0. The magnetic permeability is represented by μ_0. Because the magnitude of m_e depends on the current flowing in EM, the coefficient of the interaction can be represented as a function of the current, $\chi(I_{EM})$. In this paper, we assumed the linear relationship $\chi(I_{EM}) = \chi_0 + \chi_1 I_{EM}$. Because EM has a ferromagnetic core, an attractive force between PM and EM appears even if the current is kept to be zero. Thus χ_0 is always negative. On the other hand, the current direction changes the sign of $\chi_1 I_{EM}$. Here the current enhancing the attractive force is defined as positive. Therefore, χ_1 is also negative.

The coupling rod causes an interaction force depending on the difference of displacement of adjacent cantilevers. The force linearly changes against the displacement difference if the deformation of the rod is sufficiently small. As shown in Fig. 1 (a), the rod is attached near the support. The displacement of cantilever at the rod is quite small relative to the tip. Thus we assume the linearity of the coupling force. The whole coupled system can be excited by a voice coil motor (VCM) through the support. Therefore, the equation of motion of the coupled cantilever array is

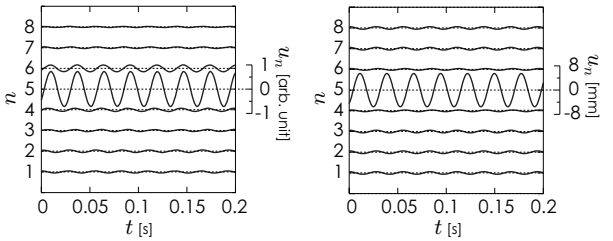

Figure 2: Intrinsic localized mode which is excited at $n = 5$. Parameters for the numerically obtained ILM are listed in Table 1. The current flowing in EMs are set at 24.0 mA.

obtained as follows:

$$\begin{cases} \dot{u}_n = v_n, \\ \dot{v}_n = -\omega_0^2 u_n - \gamma u_n + F(u_n) + A\cos(\omega t) \\ \qquad\quad - C(u_n - u_{n+1}) - C(u_n - u_{n-1}), \end{cases} \quad (2)$$

where $n = 1, 2, \ldots, 8$ and C denotes the linear inter-site coefficient. The boundary conditions of Eq. (2),

$$\begin{cases} u_0 = 0, \quad v_0 = 0, \\ u_9 = 0, \quad v_9 = 0, \end{cases} \quad (3)$$

are given by the fixed ends of cantilever array shown in Fig. 1 (a). Parameters estimated experimentally are in Table 1.

3. Observation and Manipulation

In this section, experimental results are briefly shown, focusing on the observation and the manipulation of ILM are briefly shown.

3.1. Experimentally excited ILM and numerical simulation

Intrinsic localized modes are experimentally observed when the VCM excites the macro-mechanical cantilever array at 36.1 Hz [7]. Fig. 2(a) shows waveforms of an observed ILM for each cantilever. One of the cantilevers has a quite large amplitude while the others are relatively small. The amplitude distribution is obviously localized. A numerically excited ILM is shown in Fig. 2(b). The 5th cantilever has the largest amplitude as well as the experimental one shown in Fig. 2(a). For the other ILMs, numerical simulations well match experimental observations [7]. Thus, Eq. (2) is appropriate to study ILMs.

The observed ILM is classified into "Sievers-Takeno (ST) mode" [8]. Because only one cantilever has a large amplitude relative to the others. In this paper, the observed ILM is labeled "ST5^s" to distinguish it from other coexisting ILMs, because the 5th cantilever has the largest amplitude. The detail of the naming rule is mentioned in Sec. 4.1.

3.2. Attractive Manipulation

The observed ILM does not propagate in space as long as the VCM excites the cantilever array at a constant frequency and amplitude. However, by adding an impurity

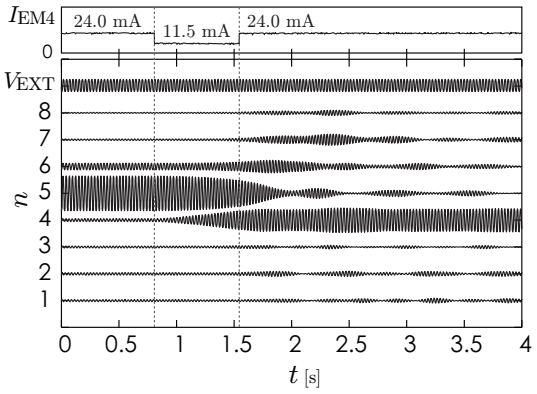

Figure 3: Manipulation of an ILM by adding an impurity. The impurity is added at $n = 4$ by varying the current I_{EM4} from 24.0 mA to 11.5 mA.

to the cantilever array, the ILM can be shifted its position. Fig. 3 shows an attractive manipulation. In this manipulation, ST5^s is initially excited. After the impurity is added, the amplitude of 4th cantilever begins to increase. On the other hand, the amplitude of 5th cantilever is decreased. The impurity is removed when the amplitudes of 4th and 5th cantilever are almost same. The oscillation of 5th cantilever becomes smaller with spreading small traveling waves. However, the amplitude of 4th cantilever grows in large. As a result, the locus of ILM is shifted from $n = 5$ to $n = 4$. That is, ST5^s is attracted to the impurity.

4. Global Phase Structure and Impurity

In this section, the mechanism of the attractive manipulation is discussed based on the phase structure.

4.1. Coexisting ILMs

By numerical simulations, many localized solutions are found in Eq. (2). In this paper, we only focus on localized solutions which exist nearby ST5^s. Figs. 4(a)–(f) shows the localized solutions which are obtained by the anticontinuous limit [9]. Even symmetric ILMs shown in Figs. 4(b) and 4(e) are called "Page (P) mode" [8]. P-modes are labeled by using two numbers because two cantilevers have a large amplitude. Then the ILM shown in Fig. 4(b) is labeled "P4^s-5^s". The upper suffix of label is based on the initial condition of the anticontinuous limit. When cantilevers in the array are decoupled, each cantilever independently oscillates. In this case, three oscillatory states are found for each cantilever at which the frequency of the external force is set at 35.7 Hz. That is, the stable resonance, the unstable resonance, and the stable antiresonance. These three states are arbitrarily chosen for an initial combination of the anticontinuous limit. For localized solutions, only one or two cantilevers are set at the stable or the unstable resonance while the others are set at the stable antiresonance. The upper suffix of ST5^s implies that the 5th cantilever is set at the stable resonance at the initial step of the anticontinuous limit. P4^u-5^u is labeled In the same manner, namely, the 4th and 5th cantilevers are set at the unstable resonance.

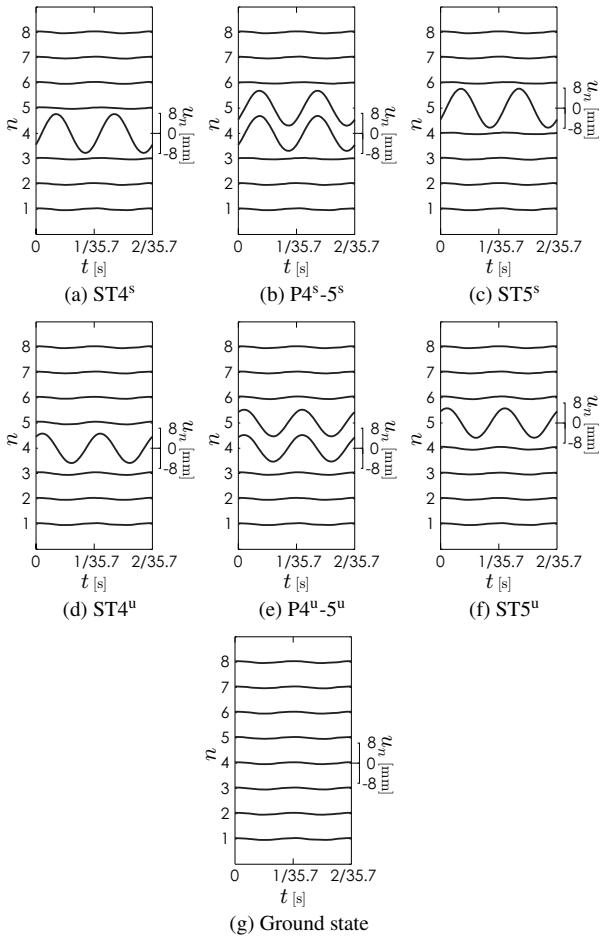

Figure 4: Numerically obtained ILMs around ST5^s. P4^u-5^s(P4^s-5^u) does not coexist for this case. It can survive if the coupling coefficient C is sufficiently small.

The stability of coexisting solutions shown in Fig. 4 is determined by Floquet multipliers. ST4^s and ST5^s are stable. The ground state shown in Fig. 4(g) is also stable. For ST4^u, ST5^u, and P4^s-5^s, one of Floquet multipliers is real and greater than +1. On the other hand, P4^u-5^u has two Floquet multipliers outside unit circle. These multipliers are also real. It implies that ST4^u, ST5^u, and P4^s-5^s have a one dimensional unstable manifold and P4^u-5^u has a two dimensional unstable manifold. In the next section, the global phase structure is discussed by calculating one dimensional unstable manifolds and domains of attraction of stable ILMs.

4.2. Unstable manifolds and domains of attraction

An impurity in the cantilever array changes the phase structure. The attractive manipulation is a result of the change of phase structure. Fig. 5 shows the phase structure when an impurity exists at $n = 4$. The impurity is induced by decreasing the current I_{EM4} to 5 mA. In Fig. 5, ST4^u, ST5^u, and P4^s-5^s survive at $I_{EM4} = 4$ mA. ST4^u, ST5^u, and P4^s-5^s are vanished by adding the impurity. ST5^s at the no-impurity regime (ST5$^s_{\mathrm{no-impuirty}}$) is indicated by the open circle. Domains of attraction are calculated for

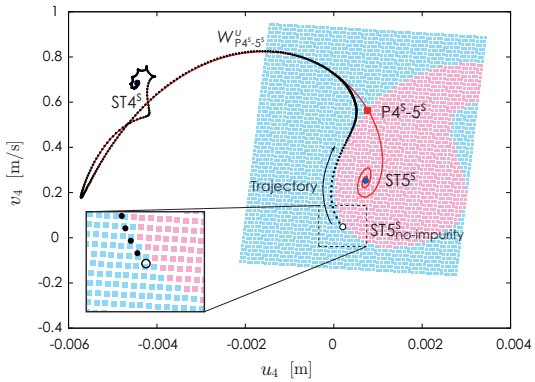

Figure 5: Phase structure around $ST5^s$ with the impurity. Solid square and circles indicate coexisting ILMs. Unstable manifolds of P4-5 are represented by solid curves. Blue and red regions correspond to domains of attraction of ST4 and ST5, respectively.

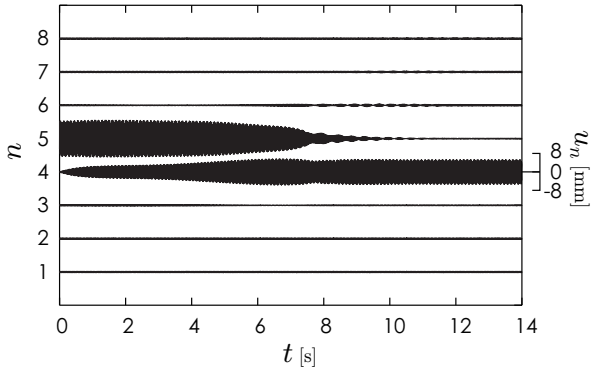

Figure 6: Numerical simulation of the attractive manipulation shown in Fig. 3. The current flowing in EM at $n = 4$ is decreased to 4 mA when the impurity is added. The impurity is added at $t = 0$. The amplitude and the frequency of external excitor are set at $A = 3$ m/s^2 and $\omega = 2\pi \times 35.7$ rad/s.

phase points on the plane which includes $P4^s$-5^s, $ST5^s$, and $ST5^s_{\mathrm{no-impuirty}}$. The blue region corresponds to the domain of attraction of $ST4^s$. In Fig. 5, the open circle is in the blue region. So, the trajectory started from the open circle converges to $ST4^s$. Fig. 6 shows waveforms of the trajectory in Fig. 5. The amplitude of 4th cantilever becomes almost same as the 5th cantilever around $t = 6$. Then the oscillation of 4th cantilever glows in large and the oscillation of 5th cantilever becomes smaller. Consequently, $ST5^s$ is attracted by the impurity as well as the experimental result.

The blue region in Fig. 5 tends to be large as the current I_{EM4} becomes small. That is, the impurity changes the phase structure around $ST5^s$. Therefore, it is concluded that the attractive manipulation is caused as a result of the change of phase structure.

5. Concluding Remarks

The macro-mechanical cantilever array was produced to study the dynamics of intrinsic localized mode. In this paper, the attractive manipulation was experimentally demonstrated and numerically discussed. As a result, the mechanism of manipulation of ILM could be investigated based on the phase structure.

The macro-mechanical cantilever array makes it easy to investigate the control of ILMs in microscopic engineering if the scaling law is held. Results in the cantilever array can be applied into micro- or nano-scale localization dynamics through the nondimensionalization of equations. We will attempt to investigate the possibility to apply the analysis using the macro-mechanical cantilever array for micro-engineering.

Acknowledgments

This research was supported by Kyoto University Venture Business Laboratory (VBL), Grant-in-Aid for Young Scientists and the Global-COE Program of Kyoto University.

References

[1] A. J. Sievers and S. Takeno, "Intrinsic localized modes in anharmonic crystals," *Phys. Rev. Lett.*, vol.61, p.970, 1988.

[2] M. Sato, B. E. Hubbard, A. J. Sievers, B. Ilic, D. A. Czaplewski, and H. G. Craighead, "Observation of locked intrinsic localized vibrational modes in a micromechanical oscillator array," *Phys. Rev. Lett.*, vol.90, p.044102, 2003.

[3] M. Sato, B. E. Hubbard, and A. J. Sievers, "*Colloquium*: Nonlinear energy localization and its manipulation in micromechanical oscillator arrays," *Rev. Mod. Phys.*, vol.78, p.137, 2006.

[4] Philip S. Waggoner and Harold G. Craighead, "Micro- and nanomechanical sensors for environmental, chemical, and biological detection," *Lab Chip*, vol.7, p.1238, 2007.

[5] M. Sato, B. E. Hubbard, A. J. Sievers, B. Ilic, and H. G. Craighead, "Optical manipulation of intrinsic localized vibrational energy in cantilever arrays," *Europhys. Lett.*, vol.66, (3) p.318, 2004.

[6] T. Hikihara, Y. Okamoto, and Y. Ueda, "An experimental spatio-temporal state transition of coupled magneto-elastic system," *Chaos*, vol.7, p.810, 1997.

[7] M. Kimura and T. Hikihara, "Coupled cantilever array with tunable on-site nonlinearity and observation of localized oscillations," *Phys. Lett. A*, vol.373, (14) p.1257, 2009.

[8] S. Flach and A. Gorbach, "Discrete breathers in Fermi-Pasta-Ulam lattices," *Chaos*, vol.15, p.15112, 2005.

[9] L. M. Marín and S. Aubry, "Breathers in nonlinear lattices: numerical calculation from the anticontinuous limit," *Nonlinearity*, vol.9, p.1501, 1996.